Isoform-Specific Localization of *Brassica rapa* Nitrilases in Root Infected with *Plasmodiophora brassicae* Revealed Using In Situ Hybridization Probes Improved with Locked Nucleic Acids

Toshiki Ishikawa · Keiichi Okazaki · Tomohiko Nagaoka · Kimiko Itoh · Toshiaki Mitsui · Hidetaka Hori

Abstract We established an in situ hybridization (ISH) technique by modification of hybridization probes with locked nucleic acids (LNAs) and demonstrated isoform-specific localization of transcripts of *Brassica rapa nitrilase* (*BrNIT-T*) genes in clubroot tissue infected with *Plasmodiophora brassicae*. Chimeric oligo DNA probes containing LNAs demonstrated highly improved specificities and could discriminate between *BrNIT-T1* and *BrNIT-T2*. These LNA-containing probes were applied to ISH. *BrNIT-T1* was strongly expressed in cells containing expanding secondary plasmodia of *P. brassicae*, but not in cells containing resting spores. On the other hand, *BrNIT-T2* transcripts were localized in noninfected cells rather than infected cells during the clubroot growth phase but coexisted with mature resting spores at a later phase of clubroot development. Immunostaining for indole-3-acetic acid (IAA) revealed IAA accumulation in cells containing growing plasmodia. IAA immunostaining in infected cells was reduced as the pathogen formed resting spores, but the signal was again enhanced in cells containing mature resting spores at a later phase of infection, suggesting that IAA is involved in both the early growth and the latest maturation phase of clubroot development. Expression of *BrNIT-T1* and *BrNIT-T2* in turnip roots was upregulated by exogenous treatment with cytokinin and jasmonic acid, respectively. Thus, these two phytohormones are possible triggers of abnormal IAA production in clubroot tissue via induction of the respective nitrilase. Given these results, we propose a model for isoform-specific roles of *B. rapa* nitrilases in auxin biosynthesis involved in phytohormone crosstalk during development of clubroot disease.

Keywords *Brassica rapa* L. (turnip) · Clubroot disease · Indole-3-acetic acid (IAA) · In situ hybridization (ISH) · Locked nucleic acid (LNA) · Nitrilase · *Plasmodiophora brassicae*

T. Ishikawa · K. Okazaki · T. Nagaoka · K. Itoh · T. Mitsui · H. Hori (✉)
Laboratories of Applied Bioscience, Institute of Science and Technology, Niigata University, Niigata 950-2181, Japan
e-mail: hide-hri@gs.niigata-u.ac.jp

T. Ishikawa
e-mail: toishika@mail.saitama-u.ac.jp

Present Address:
T. Ishikawa
Graduate School of Science and Engineering, Saitama University, Saitama 338-8570, Japan

Introduction

Plasmodiophora brassicae parasitizes roots of cruciferous plants and induces abnormal division and expansion of the infected cells, resulting in root hypertrophy known as clubroot. To control this disease, it is necessary to understand the molecular mechanisms of clubroot formation and pathogen growth. Auxin and cytokinin (CK) are believed to be essential for clubroot formation. The pathogen itself can synthesize CK (Dekhuijzen 1981; Müller and Hilgenberg 1986) but not auxin, to our knowledge. It is generally accepted that observed upregulation of plant auxin biosynthetic enzymes upon *P. brassicae* infection supplies sufficient auxin for pathogen needs (Grsic-Rausch and others 2000; Ando and others 2006; Ishikawa and others 2007b), although the accurate pathway(s) for auxin synthesis in clubroot tissues remains elusive.

Nitrilase is one of the enzymes involved in production of the auxin indole-3-acetic acid (IAA) in Brassicaceae. Although Brassicaceae nitrilases show poor substrate

preference for the IAA precursor indole-3-acetonitrile (IAN) in vitro (Bestwick and others 1993; Vorwerk and others 2001; Ishikawa and others 2007b), a role in the in vivo production of IAA has been supported by the fact that the *Arabidopsis nit-1* mutant, deficient in the predominant nitrilase isoform AtNIT1, is resistant to exogenous treatment with physiological concentrations of IAN, which normally inhibit root growth as effectively as treatment with IAA (Normanly and others 1997). Initiation and progression of clubroot are suppressed in the *nit-1* mutant and in transgenic *Arabidopsis* expressing antisense *NIT* (Grsic-Rausch and others 2000; Neuhaus and others 2000), strongly indicating that nitrilase has a vital role in clubroot disease in *Arabidopsis*. In addition, the dependency of clubroot growth on NIT1 activity implies that *P. brassicae* is unable to produce sufficient auxin for clubroot development, even if the pathogen possesses auxin-producing ability.

Increased nitrilase activity has been observed in clubroot tissues of agricultural varieties of *Brassica*, namely, *B. rapa* (Chinese cabbage and turnip) and *B. napus* (rutabaga) (Rausch and others 1981; Grsic and others 1999; Ugajin and others 2003), but these studies did not demonstrate a direct involvement of nitrilase at the mRNA level (Bischoff and others 1995; Grsic and others 1999). In addition, increased nitrilase activity in *B. rapa* cultivars was observed only at a late phase of clubroot development. On the other hand, Ando and others (2006) reported that the expression and activity of indole-3-acetaldehyde oxidase were enhanced from an early phase of clubroot development in Chinese cabbage. Thus, these findings may neglect the involvement of nitrilase at an early phase of clubroot formation.

In contrast, our recent work indicated the involvement of nitrilase in an early phase of disease development in turnip. We isolated three turnip nitrilases and showed that expression of *BrNIT-T1* and *BrNIT-T2*, encoding nitrilases that produce IAA, was differentially regulated throughout clubroot disease development (Ishikawa and others 2007b). In particular, *BrNIT-T1* expression was highly elevated during the early stage of clubroot development, indicating that this isoform is specifically involved in IAA synthesis during initiation of clubroot. However, the role of *BrNIT-T1* in IAA synthesis remains elusive for two reasons: (1) the increased expression of *BrNIT-T1* in infected tissues was lower than or comparable to the constitutive expression level of *BrNIT-T2*, the predominant nitrilase in turnip roots, and (2) recombinant turnip nitrilases showed poor preference for IAN compared to other natural nitrile compounds (Ishikawa and others 2007b). Therefore, to confirm associations between *P. brassicae* development, *BrNIT-T* expression, and IAA synthesis in clubroot tissue, we investigated the distribution of nitrilase transcripts and

IAA in clubroot tissues. In addition, we evaluated the regulatory effects of exogenous treatment with phytohormones on *BrNIT-T* expression. Our results suggest that plant hormone–regulated expression of *BrNIT-T* isoforms is necessary for clubroot initiation and progression.

Materials and Methods

Plant Growth and Pathogen Inoculation

Plants were cultivated and inoculated as described previously (Ishikawa and others 2007b). Seeds of the turnip *Brassica rapa* L. cv. Natsumaki 13-gou kokabu (The Musashino Seed Co., Ltd., Tokyo, Japan) were grown on soil in a pot at 24°C under a 9-h dark/15-h light regimen at a photon flux density of 130 μmol m^{-2} s^{-1}. One day after germination (dag), each seedling was inoculated with 1 ml of *P. brassicae* resting-spore suspension (10^7–10^8 spores/ml). Control plants were not treated with spores. Plants were harvested at designated time points and used for the experiments below.

RNA Extraction, cDNA Generation, and Semiquantitative RT-PCR Analysis

Total RNA was prepared as described previously (Ishikawa and others 2007b). Reverse transcription and PCR were performed using the PrimeScript RT reagent kit and *ExTaq* polymerase (Takara Bio Inc., Kyoto, Japan) according to the manufacturer's protocols. Primer sequences are listed in Table 1. PCR was performed using a DICE thermal cycler (Takara Bio Inc.). Following a primary denaturation step for 30 s at 96°C, 23–32 cycles were carried out with 10-s denaturation at 96°C, 20-s annealing at 60/60/65/61°C (*BrNIT-T1/BrNIT-T2/BrNIT-T4/β-actin*, respectively), and extension at 72°C for 12/8/10/10 s (*BrNIT-T1/BrNIT-T2/BrNIT-T4/β-actin*, respectively). PCR products were analyzed by native PAGE with a 4% stacking gel (pH 6.8) and a 9% separating gel (pH 8.8) in Tris-glycine running buffer (Laemmli 1970). *β-Actin* was amplified in separate reactions as the internal reference.

Probe Preparation

Digoxigenin (DIG)-labeled RNA probes were prepared using a DIG RNA Labeling kit (Roche Diagnostics, Basel, Switzerland). The 3′ untranslated regions of *BrNIT-T1* and *BrNIT-T2* were amplified using PCR primers (Table 2) and cloned into the *Eco*RV site of pBluescript II SK(+). The cloned fragments were excised from the vector by double digestion with *Hin*dIII and *Eco*RI and subcloned into the pSPT18 or pSPT19 vector (Roche Diagnostics). RNA

Table 1 Primer sequences used for quantitative PCR analyses

Gene	Primer sequences (5′ → 3′)	Amplicon (bp)
BrNIT-T1	Forward: TCCATTGGGAAAGATCCTC	273
	Reverse: GAGAAGGGAGACGATAGATTGA	
BrNIT-T2	Forward: AAGTAACCAAAGATATAAAGGTCCTCTC	163
	Reverse: CAGACAACGCAGATCAAACCA	
BrNIT-T4	Forward: AGAGAGCCTCACACCGGACT	227
	Reverse: TAACCGCTTTCCTCGGGTGC	
β-Actin	Forward: TGGAGAAGATCTGGCATCACAC	223
	Reverse: ATCACCAGAATCCAGCACAATACC	

Table 2 Oligonucleotides used for in situ hybridization

Gene	Primer sequences (5′ → 3′)		Location
PCR primers for in vitro transcription template preparation			
BrNIT-T1	Forward: AGGTCGTTGTCAATCTATCGT		1088–1326
	Reverse: GGTCCACACGTTAAAACATAAC		
BrNIT-T2	Forward: AGTAACCAAAGATATAAAGGTCCTCTC		1088–1329
	Reverse: GATACTTAAAACATTATTTCAACC		
Gene	Oligo sequences (5′ → 3′)[a]	T_m[b]	Location
LNA-modified DNA probes			
BrNIT-T1	GTAcatatccaacTGgCtctcGTTG	82	1224–1248
BrNIT-T2	AACcatatccaacCAgGtctcTCA	78	1211–1234

[a] LNA nucleotide in uppercase and DNA nucleotide in lowercase

[b] Predicted using the Exiqon T_m prediction tool (http://lna-tm.com/) at 300-mM salt concentration and 0.1-µM probe concentration (in hybridization buffer)

probes were generated using T7 or SP6 RNA polymerase according to the manufacturer's protocol.

Modified oligodeoxynucleotide probes containing locked nucleic acids (LNAs) were designed (Table 2) with a DIG label at the 3′ end and purchased from Greiner Bio-One GmbH (Frickenhausen, Germany).

Evaluation of Probe Specificity

To confirm the specificity of RNA probes as well as LNA-modified DNA probes, probes were applied to dot-blot hybridization with synthesized RNA. The full-length RNAs of BrNIT-T1 and BrNIT-T2 were generated in the sense direction using T7 RNA polymerase and DIG-free nucleotides. After digestion of plasmid templates by DNase I and purification by ethanol precipitation, 0.1 ng of the sense RNA was dot-blotted on a nylon membrane (Hybond-N+, GE Healthcare UK Ltd., Buckinghamshire, England) and UV crosslinked. The membrane was prehybridized in high-SDS hybridization buffer [5× SSC (150 mM NaCl and 15 mM sodium citrate, pH 7.0, at 1× concentration), 0.1% (w/v) N-lauroylsarcosine, 2% (w/v) blocking reagent (Roche Diagnostics), 7% (w/v) SDS, 20 µg ml^{-1} denatured salmon sperm DNA, 50% (v/v) formamide] for 2 h at 50°C with gentle rotation. Hybridization was performed by adding probes at 80 ng ml^{-1} for RNA probes or at 0.4 pmol ml^{-1} for LNA probes and incubating at 50°C for 12 h. The membrane was rinsed with 2× SSC containing 0.1% (w/v) SDS at room temperature and washed three times with 2× SSC/50% (v/v) formamide for 30 min each at 50°C with gentle rotation. DIG was visualized using the DIG Nucleic Acid Detection kit (Roche Diagnostics) according to the manufacturer's instructions.

In Situ Hybridization (ISH)

All steps were carried out at room temperature unless otherwise stated. Fresh turnip tissues were cut into 2–5-mm pieces and fixed overnight at 4°C with 4% (w/v) paraformaldehyde and 0.25% (w/v) glutaraldehyde in PBS supplemented with 0.03% (v/v) Tween 20. The tissues were then dehydrated sequentially with a water/ethanol/t-butanol series as follows: 50/40/10, 30/50/20, 10/55/35, 0/50/50, and 0/25/75 (v/v), and then three times with absolute t-butanol (1 h each). Tissues were infiltrated and embedded in Paraplast Plus (Sigma, St. Louis, MO). Sections (10 µm) were stretched on MAS-coated slides (Matsunami Glass Ind., Ltd., Tokyo, Japan), deparaffinized in xylene, and

hydrated in an ethanol/water series. The sections were then treated sequentially with 0.2 N HCl for 10 min, 1 μg ml^{-1} proteinase K (Sigma) for 10 min at 37°C, 4% (w/v) paraformaldehyde in PBS for 10 min, and 0.5% (v/v) acetic anhydride in 0.1 M triethanolamine (pH 8.0) twice for 5 min. The sections were vigorously washed with water several times, dehydrated with a water/ethanol series, and air-dried.

Hybridization was performed using the specific probes prepared as above at 0.1–0.4 μM in hybridization buffer [10 mM Tris–HCl (pH 7.5), 0.3 M NaCl, 5 mM EDTA, 50% (v/v) formamide, 10% (w/v) dextran sulfate, 1× Denhardt's solution, 0.25% (w/v) SDS, 500 μg ml^{-1} yeast tRNA, 500 μg ml^{-1} denatured salmon sperm DNA] for 16 h at 50°C. The slides were washed once with 4× SSC for 15 min at 50°C and three times with 2× SSC containing 50% (v/v) formamide for 60 min at 50°C. When RNA probes were used, the specimens were treated with 20 μg ml^{-1} RNase A for 30 min at 37°C between the second and third washes with 2× SSC/50% formamide. Target signals were visualized using the Roche DIG Nucleic Acid Detection kit. After staining, the specimens were mounted and photographed under a microscope. For negative controls, sense RNAs of both *BrNIT-T1* and *BrNIT-T2* (*NIT1^{RNA}* and *NIT2^{RNA}*) were mixed and used for hybridization.

Immunostaining for IAA

Histochemical analysis of IAA distribution was performed according to Moctezuma's method (Moctezuma 1999), with several modifications as described below. Anti-IAA monoclonal antibody was purchased from Agdia Inc. (Elkhart, IN, USA). Tissues were prefixed with 3% (w/v) 1-ethyl-3-(dimethylaminopropyl)carbodiimide for 1 h at 4°C and then fixed in 4% (w/v) paraformaldehyde and 2.5% (w/v) glutaraldehyde in PBS overnight at 4°C. After dehydration in a water/ethanol series, tissues were embedded in polyester wax (Electron Microscopy Sciences, Hatfield, PA, USA) at 38°C and cut into 8-10-μm-thick sections. The sections were treated with xylene to remove wax and hydrated as described above. Slides were incubated for 45 min in blocking solution [10 mM sodium phosphate (pH 7.4) containing 0.1% (v/v) Tween 20, 1.5% (w/v) glycine, and 5% (w/v) bovine serum albumin (BSA)] and then rinsed briefly with regular salt rinse solution (RSR) [10 mM sodium phosphate (pH 7.4) containing 0.1% (v/v) Tween 20, 0.8% (w/v) BSA, and 0.88% (w/v) NaCl] for 5 min, followed by PBS containing 0.8% (w/v) BSA (P-BSA). Sections were incubated with a 1:20 dilution of 1 mg ml^{-1} monoclonal anti-IAA in P-BSA for 6 h and washed with high-salt rinse solution [10 mM sodium phosphate (pH 7.4) containing 0.1% (v/v) Tween 20, 0.1%

(w/v) BSA, and 2.9% (w/v) NaCl] twice for 5 min, followed by a wash with RSR for 10 min. The sections were rinsed with P-BSA and incubated for 12 h with a 1:100 dilution of 1 mg ml^{-1} goat anti-mouse IgG conjugated with alkaline phosphatase (Promega, Madison, WI, USA). After rinsing twice with RSR and once with water, the specimens were incubated with Western Blue Stabilized Substrate for alkaline phosphatase (Promega). The sections were washed with water, mounted, and photographed.

Hormone Treatment

Turnip seeds were sterilized with 5% sodium hypochlorite for 10 min and washed several times thoroughly with sterile distilled water. Eight seeds were sown and cultured in 40 ml of half-strength Murashige and Skoog medium supplemented with 1% (w/v) sucrose in a 200-ml flask at 25°C and constantly rotated at 60 rpm under continuous light at 80 μmol m^{-2} s^{-1}. One week after sowing, the culture was inoculated with hormones (dimethylsulfoxide solution, 1000-fold dilution) and incubated for an additional 24 h under the same conditions. Control plants were treated with dimethylsulfoxide. Final concentrations of hormones in the medium were 100 μM IAN, 10 μM IAA, 30 μM methyl jasmonate, and 30 μM benzyladenine. Roots of the eight seedlings were pooled, and PCR analysis was performed as described below using three independent sample pools.

Real-Time PCR Analysis

Real-time PCR was performed using a Thermal Cycler Dice Real Time System (Takara Bio Inc.) and SYBR *Premix Ex Taq* (Takara Bio Inc.). PCR was carried out as follows: initial denaturation at 95°C for 30 s, 40 cycles of amplification (denaturation at 95°C for 5 s, annealing at 60°C for 15 s, extension at 72°C for 10 s), and melting temperature analysis from 72 to 95°C at a linear increase of 0.5°C s^{-1}. PCR primers (Table 2) were used at 0.2 μM each. Measurements were repeated three times using cDNAs prepared independently from different root pools. External standard curves were constructed from three independent runs using plasmid DNA carrying the target sequence.

Results

Tissue-Specific Expression of *B. rapa* Nitrilases in Healthy Turnip

We previously characterized the differential expression of *B. rapa* nitrilases during clubroot development (Ishikawa
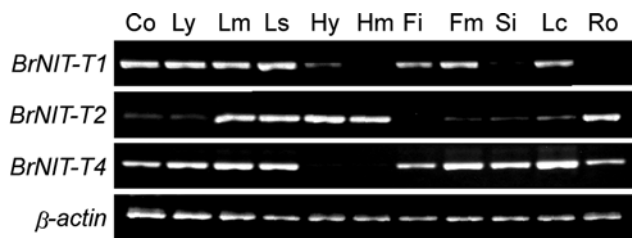
Fig. 1 Tissue localization of *BrNIT-T* transcripts. RT-PCR was performed for *BrNIT-T* (29 cycles) and *β-actin* (internal control; 26 cycles), and amplicons were analyzed by native PAGE. *Co* cotyledon; *Ly* young leaf; *Lm* mature leaf; *Ls* senescent leaf; *Hy* young hypocotyl; *Hm* mature hypocotyl; *Fi* immature flower; *Fm* mature flower; *Si* silique; *Lc* cauline leaf; *Ro* root

and others 2007b). Here, the expression of the nitrilases in various tissues was investigated by RT-PCR analysis to verify the differential regulation of their expression during turnip development. *BrNIT-T1* was expressed in most aerial parts of the plant except for the hypocotyl, that is, in the cotyledon, true leaves, and inflorescence (Fig. 1). No *BrNIT-T1* amplicon was detected from root cDNA following 29 cycles of PCR, but the amplicon was detected faintly after 32 cycles (data not shown). On the other hand, *BrNIT-T2* transcripts were abundant in the hypocotyl and root, where *BrNIT-T1* transcripts were negligible. *BrNIT-T2* was also expressed in mature and senescent leaves, whereas very little was expressed in the cotyledon, young leaves, and inflorescence. *BrNIT-T4*, a nitrilase gene encoding *β*-cyanoalanine hydratase/nitrilase, was expressed in all plant tissues except for the hypocotyl. These results clearly showed that the expression of nitrilase isoforms is regulated differentially depending on plant tissue.

Development of LNA-Modified DNA Probes

To achieve our ultimate goal of determining the cellular localization of *BrNIT-T1* and *BrNIT-T2* transcripts in *P. brassicae*-infected cells, we designed highly specific probes for ISH analysis. We prepared RNA probes for *BrNIT-T1* and *BrNIT-T2* based on their 3′ untranslated regions and confirmed their specificities by dot-blot Northern hybridization. Unfortunately, the RNA probes ($NIT1^{RNA}$ and $NIT2^{RNA}$) cross-reacted (that is, each probe recognized both full-length transcripts; Fig. 2a). These weak but clear mismatched hybridization signals did not disappear by increasing the temperature to 65°C during hybridization and washing procedures (data not shown).

To find probes that differentiate between *BrNIT-T1* and *BrNIT-T2*, we designed oligo DNA probes that had short regions with several clusters (2–3 nucleotides) of unique sequences between the two nitrilases. We had previously used such DNA oligos as PCR primers for isoform-specific amplification of *BrNIT-T* genes (Ishikawa and others
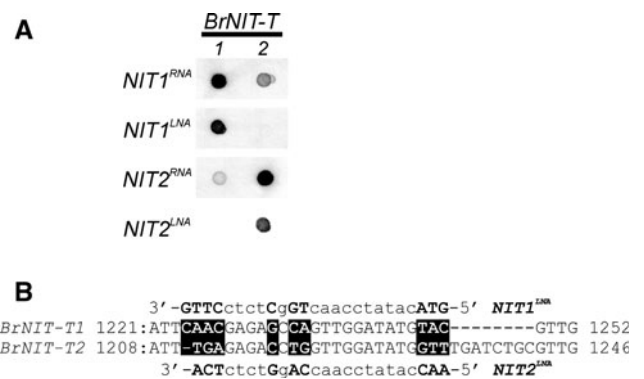

Fig. 2 Hybridization probes for in situ hybridization of *BrNIT-T* transcripts. **a** Dot-blot Northern hybridization. Full-length sense RNAs of *BrNIT-T1* and *BrNIT-T2* were spotted onto the membrane and hybridized with RNA probes ($NIT1^{RNA}$ and $NIT2^{RNA}$) and LNA-modified DNA probes ($NIT1^{LNA}$ and $NIT2^{LNA}$). **b** Sequence alignment of LNA-modified DNA probes. Highlighted letters in the partial sequences of *BrNIT-T1* and *BrNIT-T2* indicate identities. Uppercase and lowercase letters in the sequences of $NIT1^{LNA}$ and $NIT2^{LNA}$ indicate LNA and DNA nucleotides, respectively

2007b). However, because DNA oligos have low melting temperatures (T_m), they can cause nonspecific hybridization in ISH. To overcome this problem, LNAs were incorporated into the DNA probes. LNA nucleotides increase the stability of the desired duplex and result in a higher T_m. In addition, if the duplex contains a mismatch, the T_m is drastically reduced owing to the structural inflexibility of LNA. Thus, the addition of LNA nucleotides improves probe specificity by increasing the stability of the desired duplex while decreasing the stability of mismatched duplexes (Koshkin and others 1998a, b; Obika and others 1998). We selected a region that included three clusters consisting of three or four isoform-specific nucleotides, which resulted in 40% sequence dissimilarity between *BrNIT-T1* and *BrNIT-T2*, and we substituted LNA nucleotides in those positions (Fig. 2b). The substitution of 9-10 LNA nucleotides in 24-25 bases resulted in high T_m values suitable for high-stringency ISH (Table 2). The 3′ ends of the LNA-modified DNA probes ($NIT1^{LNA}$ and $NIT2^{LNA}$) were labeled with DIG for detection. These LNA probes showed no cross-hybridization between *BrNIT-T1* and *BrNIT-T2* as determined by dot-blot hybridization (Fig. 2a).

Isoform Specificity of LNA Probes in ISH

To further evaluate isoform specificity, both the RNA and LNA probes were used for ISH in healthy and *P. brassicae*-infected turnip roots. In healthy roots, similar staining patterns were obtained at all time points examined (15, 20, 30, and 40 dag). Typical results obtained in healthy root tissues at 20 dag are shown in Fig. 3. The $NIT1^{LNA}$ signal

Fig. 3 Probe specificity in in situ hybridization of *BrNIT-T* transcripts in healthy turnip roots. Cross sections of healthy roots at 20 dag were hybridized with *NIT1^LNA* (**a, b**), *NIT1^RNA* (**c, d**), *NIT2^LNA* (**e, f**), *NIT2^RNA* (**g, h**), and a sense probe mix (**i, j**). The boxed area in each left-hand image was magnified 5× on the right. *Red arrowheads* indicate typical signals. *C* cortex; *Ep* epidermis; *LR* lateral root-forming site; *Pr* pericycle; *Px* primary xylem; *Sx* secondary xylem; *Vc* vascular cambium. Scale bars = 500 μm (*left*) and 100 μm (*right*)
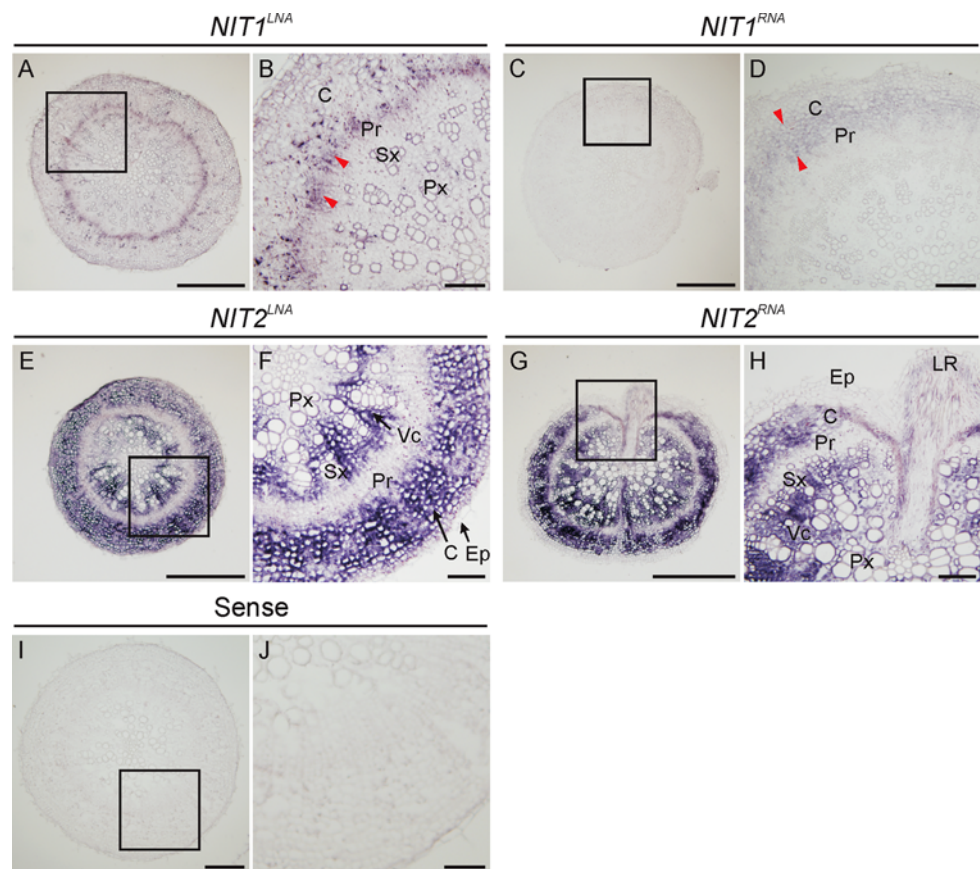
was clearly visualized in the pericycle, whereas the *NIT1^RNA* signal was observed between the pericycle and the inner parts of the cortex (Fig. 3a–d). On the other hand, far stronger signals were observed in the cortex and vascular cambium using *NIT2^LNA* and *NIT2^RNA* (Fig. 3e–h). The signal intensities of *BrNIT-T1* and *BrNIT-T2* were consistent with the results of RT-PCR analysis in healthy root (Fig. 1). Notably, the region stained using *NIT1^RNA* seemed to correspond to that stained using *NIT2^LNA* and *NIT2^RNA* rather than that stained using *NIT1^LNA*, indicating that *NIT1^RNA* cross-hybridized to *BrNIT-T2* transcripts during ISH, as observed during dot-blot hybridization (Fig. 2). Control hybridizations using mixed sense probes did not yield any signals in healthy root sections (Fig. 3i, j).
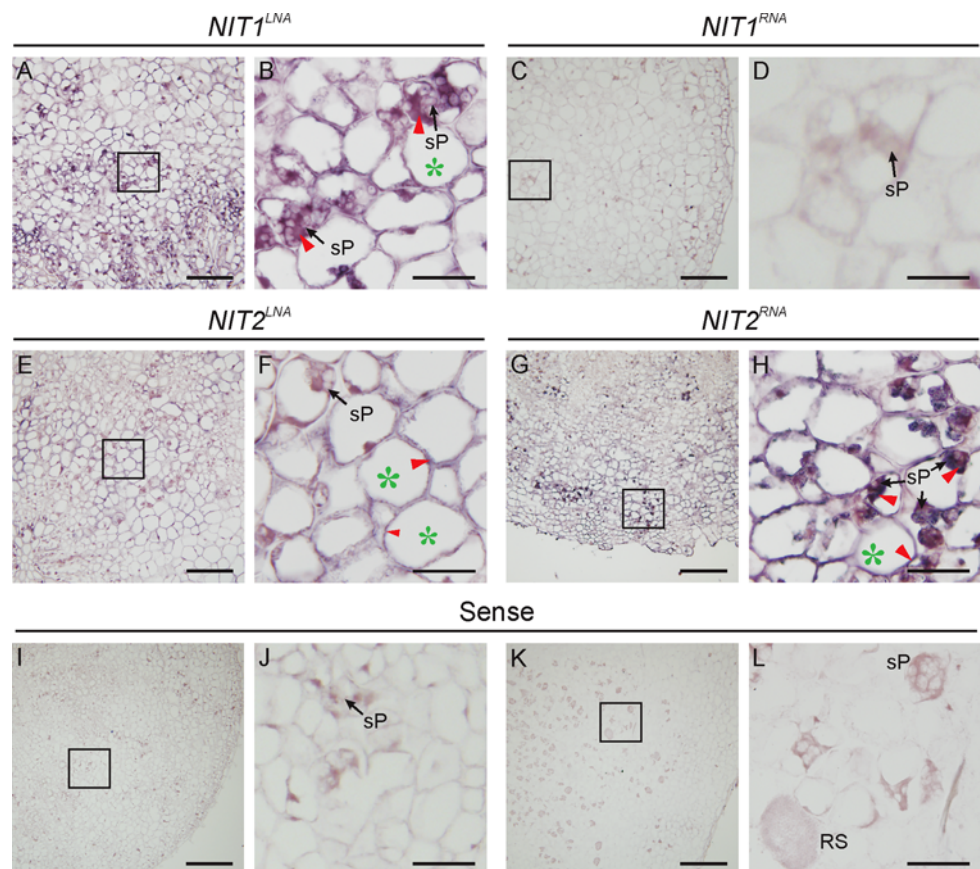
In sections from *P. brassicae*-infected roots, small secondary plasmodia of *P. brassicae* were observed in infected roots, and cell expansion was initiated at 15 dag (for example, Fig. 4a–j), before visible swelling of whole infected roots at 20 dag. Linear growth of the infected roots was sustained up to 30 dag, at which time most secondary plasmodia were enlarged in the infected cells and formation of resting spores was initiated (for example, Fig. 4k, l).

The pathogen (secondary plasmodia and resting spores) and pathogen-containing cells were faintly stained by ISH

using sense probes (Fig. 4i–l). This staining was also observed in control experiments in which probes were omitted (data not shown), indicating that the signal resulted from nonspecific hybridization. In contrast, the positive signals derived from the *NIT* probes were dark brown to blue, clearly distinguishable from background.

The *NIT1^LNA* signal in noninfected roots was restricted to pericycle (Fig. 3a, b), whereas the probe stained a wider region of infected roots at 15 dag (Fig. 4a, b). In particular, the *NIT1^LNA* staining appeared to be restricted to cells containing plasmodia (Fig. 4b). In contrast, the *NIT1^RNA* signal was very faint and indistinguishable from the background (Fig. 4c, d). Compared to the dense signals for *BrNIT-T2* in healthy roots (Fig. 3e–h), both the *NIT2^LNA* and *NIT2^RNA* signals were significantly diminished over the entire region of the infected roots (Fig. 4e–h). There was, however, a clear difference between the signals from the two *NIT2* probes in the infected roots: the *NIT2^LNA* signal was observed in pathogen-free cells but not in pathogen-containing cells (Fig. 4e, f), and the *NIT2^RNA* signal was observed in both pathogen-containing and pathogen-free cells (Fig. 4g, h). The *NIT2^RNA* staining pattern overlapped that of both *NIT1^LNA* and *NIT2^LNA*, indicating that *NIT2^RNA* cross-hybridized to the abundant *BrNIT-T1* transcripts found in pathogen-containing cells.

Taken together, the regions stained using the two LNA-modified probes were clearly distinct in both noninfected and infected roots, supporting their isoform specificities as assessed by dot-blot hybridization (Fig. 2a). In addition, the relative signal intensities (of *BrNIT-T1* versus *BrNIT-T2* and of healthy versus infected roots) parallel the results of our RT-PCR analyses (Fig. 1: *BrNIT-T2* was expressed much more strongly than *BrNIT-T1* in healthy roots) and our previous report (Ishikawa and others 2007b) (in the early-growing clubroot, *BrNIT-T1* and *BrNIT-T2* were upregulated and downregulated, respectively). These results clearly confirmed that the LNA-modified probes were suitable for comparative ISH analyses for localizing *BrNIT-T1* and *BrNIT-T2*.

LNA-Modified Probes Reveal Differential Localization of *BrNIT-T1* and *BrNIT-T2* Transcripts in Clubroot Tissues

Using the isoform-specific LNA-modified probes, we analyzed the localization of *BrNIT-T* transcripts in clubroot tissues throughout disease development. The results of ISH using *NIT1^{LNA}* and *NIT2^{LNA}* probes are shown separately in Figs. 5 and 6, respectively, at the same magnification as the healthy root controls.

At all ages examined, *BrNIT-T1* expression in healthy roots was restricted to the pericycle and the lateral root-forming region (Fig. 5a, b, e, f, i, j). In contrast, the *BrNIT-T1* staining pattern in infected roots was temporally regulated. In infected roots at 20 dag, when cells were expanded and the root architecture was disrupted, *BrNIT-T1* expression extended to most cells in infected tissues, although the signals were stronger in cells containing *P. brassicae* plasmodium than in pathogen-free cells (Fig. 5c, d). At 30 dag, the *NIT1^{LNA}* signal intensity was diminished in pathogen-free cells but was still strong in cells containing secondary plasmodia (Fig. 5g, h). Notably, the accumulation of *BrNIT-T1* transcripts was observed in cells containing secondary plasmodia but not in cells containing resting spores (Fig. 5h). At 40 dag, *BrNIT-T1* expression was observed only in cells with secondary plasmodia, not in pathogen-free cells or in cells with resting spores (Fig. 5k, l).

At all time points, the *NIT2^{LNA}* signals in healthy control roots were strong in the cortex and vascular cambium but not in lateral root-forming sites (Fig. 6a, b, e, f, i, j). On the other hand, the signal intensity in infected roots decreased significantly at 20 dag (Fig. 6c, d). In addition, the predominant signal in infected tissue was observed in pathogen-free cells rather than in pathogen-containing cells (Fig. 6d). The distribution pattern of *BrNIT-T2* transcripts was similar at 30

Fig. 5 In situ hybridization of *BrNIT-T1* using LNA-modified DNA probes in clubroot-diseased turnip roots. Cross sections of noninfected control and *P. brassicae*-infected turnip roots at 20–40 dag were hybridized with *NIT1^LNA*. The boxed area in each left-hand image was magnified 5× on the right. *Red arrowheads* indicate typical signals; *green asterisks* indicate pathogen-free cells. *C* cortex; *LR* lateral root-forming region; *Pr* pericycle; *RS* resting spores; *sP* secondary plasmodium; *Sx* secondary xylem. Scale bars = 100 μm (*left*) or 20 μm (*right*)
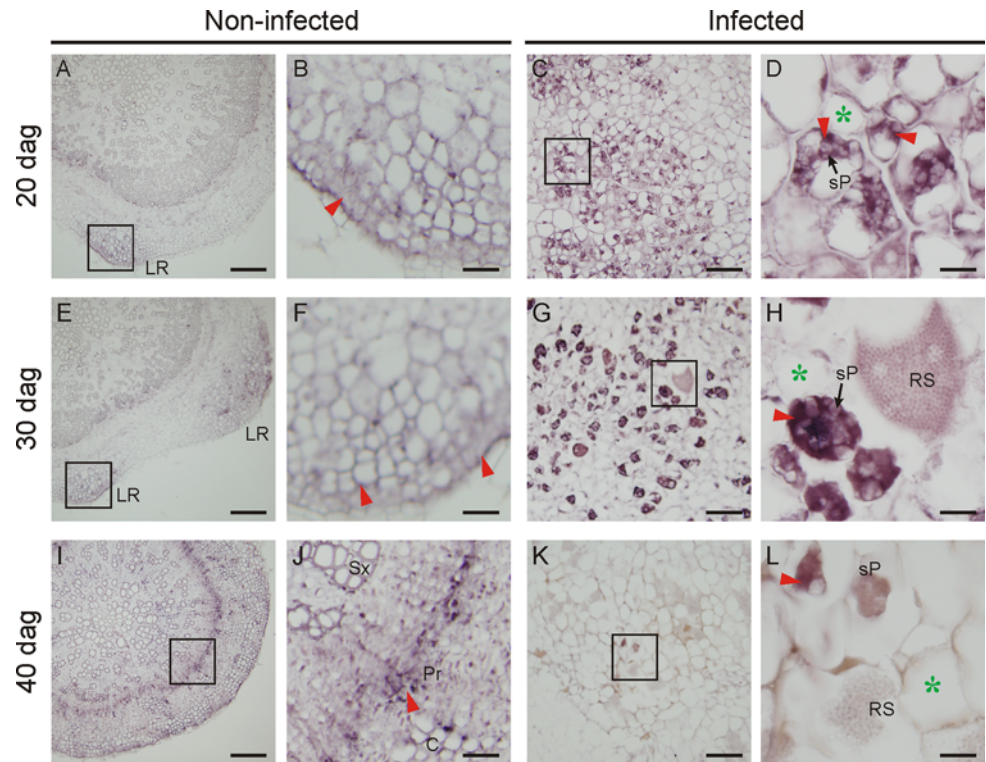
Fig. 6 In situ hybridization of *BrNIT-T2* using LNA-modified DNA probes in clubroot-diseased turnip roots. Cross sections of noninfected control and *P. brassicae*-infected turnip roots at 20-40 dag were hybridized with *NIT2^LNA*. The boxed area in each left-hand image was magnified 5× on the right. *Red arrowheads* indicate typical signals; *green asterisks* indicate pathogen-free cells. *C* cortex; *Ep* epidermis; *LR* lateral root forming region; *Pr* pericycle; *RS* resting spores; *sP* secondary plasmodium; *Sx* secondary xylem; *Vc* vascular cambium. Scale bars = 100 μm (*left*) or 20 μm (*right*)
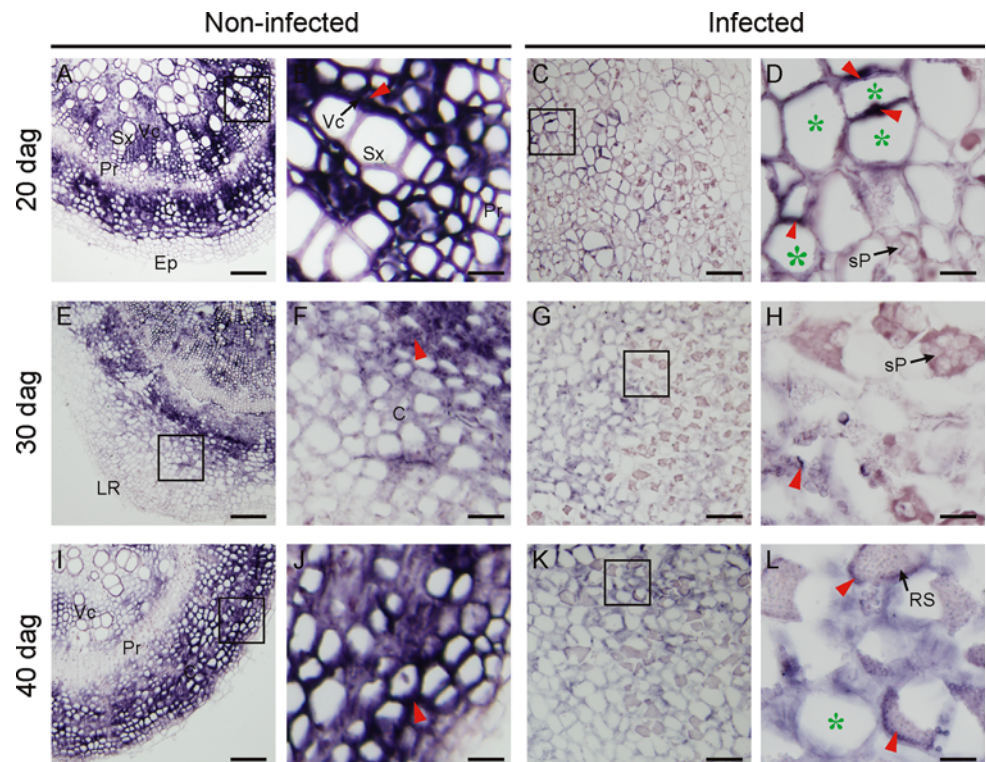
Fig. 7 Immunostaining of IAA in healthy and clubroot-diseased turnip roots. Cross sections of healthy and clubroot-diseased turnip roots were immunostained without (−Ab) or with (+Ab) monoclonal anti-IAA. Photographs **m–o** are 5× magnifications of boxed areas in **j–l**. *Red arrowheads* indicate typical signals; *asterisks* indicate noninfected cells. *C* cortex; *Ep* epidermis; *LR* lateral root-forming site; *Pr* pericycle; *RS* resting spores; *sP* secondary plasmodium; *Vc* vascular cambium. Scale bars 100 μm
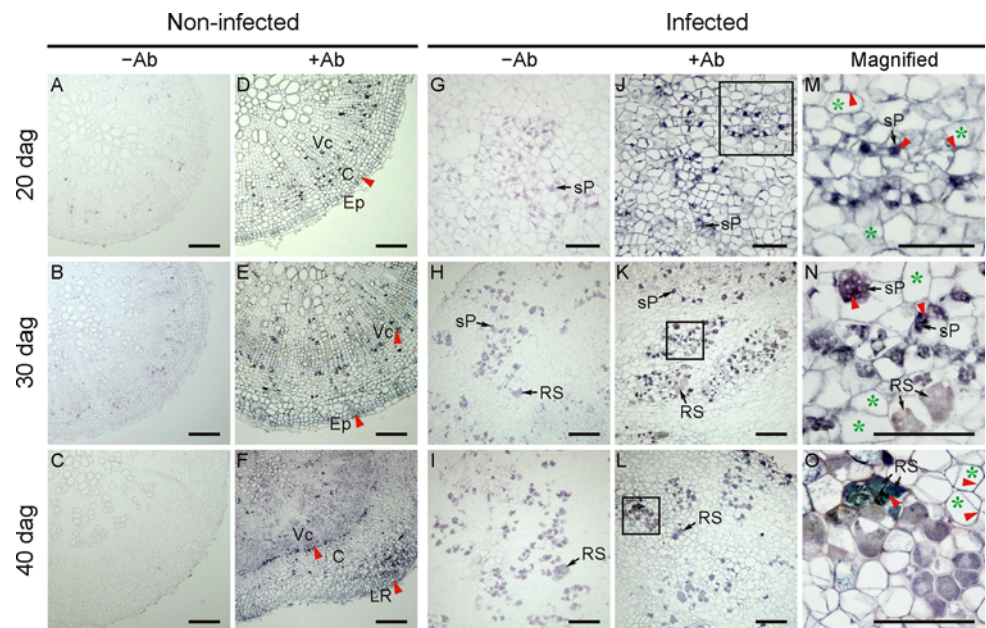
dag (Fig. 6g, h). At 40 dag, however, *BrNIT-T2* expression recovered throughout the infected tissues, even in cells containing mature resting spores (Fig. 6k, l).

Localization of IAA

In situ localization of IAA was analyzed by immunostaining using monoclonal anti-IAA (Fig. 7). In healthy roots, IAA immunostaining was observed between the outer pericycle and inner cortex, and in the outer layers of the cortex (Fig. 7d, e). The lateral root-forming region also showed a strong signal (Fig. 7f). All other cells were stained weakly, with blue-green color along the cell wall. Negative controls did not show staining (Fig. 7a–c). These IAA immunostaining patterns were constant over root age.

In infected roots at 20 dag all cortex cells were stained, and the signal was especially concentrated in infected cells and the neighboring cells (Fig. 7j, m). At 30 dag, cells without pathogen lacked IAA signal, but those containing plasmodia retained a high signal intensity (Fig. 7k, n). Notably, for infected cells at 30 dag the signal was stronger in cells containing young plasmodia than in cells containing expanded plasmodia, and no signal was detected in cells containing resting spores (Fig. 7n). At 40 dag, the IAA signal was observed in noninfected cells and was very strong in some cells containing resting spores (Fig. 7l, o).

Effects of Phytohormones and Related Compounds on Expression of *BrNIT-T* Genes

To address the regulation of expression of *B. rapa* nitrilases, young turnip seedlings were treated with various phytohormones, and the levels of *BrNIT-T* transcripts were
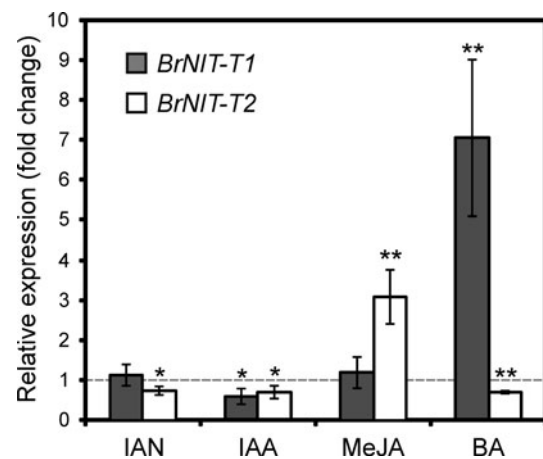
Fig. 8 Effects of hormones on *BrNIT-T* expression. Turnip roots were treated with indole-3-acetonitrile (IAN, 100 μM), indole-3-acetic acid (IAA, 10 μM), methyl jasmonate (MeJA, 30 μM), or benzyladenine (BA, 30 μM) for 24 h, and *BrNIT-T* expression was analyzed by RT-PCR. Transcript levels were represented as relative values to the dimethyl sulfoxide-treated control (indicated by *dotted line*). Data are mean ± SD ($n = 3$). *Asterisks* indicate statistical significance compared to control (Student's *t* test; *$p < 0.05$, **$p < 0.01$)

quantified by real-time PCR (Fig. 8). Treatment with IAN (100 μM) decreased *BrNIT-T2* transcripts by 73% compared to untreated controls, but IAN treatment had no effect on the level of *BrNIT-T1* transcripts. On the other hand, treatment with IAA (10 μM) decreased expression of both *BrNIT-T1* (60%) and *BrNIT-T2* (71%). Treatment with benzyladenine (30 μM) upregulated *BrNIT-T1* expression sevenfold but decreased *BrNIT-T2* expression to 70%. Treatment with methyl jasmonate (30 μM) enhanced *BrNIT-T2* expression up to threefold but *BrNIT-T1* was unaffected.

Discussion

Increased Specificity of ISH Probes by Incorporation of LNAs

We recently isolated two analogous nitrilases genes, *BrNIT-T1* and *BrNIT-T2*, involved in IAA biosynthesis in turnip (Ishikawa and others 2007b). Despite the similar enzymatic characteristics of their recombinant proteins, the nitrilases are differentially expressed during clubroot development. Furthermore, RT-PCR analysis in the present study demonstrated distinct expression patterns of *BrNIT-T1* and *BrNIT-T2* in healthy turnip tissues (Fig. 1). These results suggest isoform-specific physiological roles of the nitrilases in normal turnip growth as well as clubroot disease development.

In the present study we aimed to determine whether the cellular distribution of the *BrNIT-T* transcripts correlates with clubroot pathogen in diseased tissues. Although ISH analysis using traditional RNA probes failed to discriminate between *BrNIT-T1* and *BrNIT-T2* because of their high degree of similarity, the subsequent use of LNA-modified DNA probes permitted isoform-specific detection. As described above, LNAs increase stability of the accurate duplex and instability of the mismatched duplex. Taking advantage of this unique property, LNA probes have been utilized for single nucleotide polymorphism and microRNA studies, including ISH (Simeonov and Nikiforov 2002; Silahtaroglu and others 2004; Válóczi and others 2004, 2006). The LNA-modified DNA probes for *BrNIT-T1* and *BrNIT-T2* were designed based on regions of their 3′ untranslated region sequences that include several differences between the two nitrilases (Fig. 2b). The LNA-modified probes had high T_m values despite their short length (Table 2), leading to a large difference in temperature stability between the completely complementary duplex and a mismatched duplex. In Northern dot blots, the LNA probes did not hybridize to inappropriate nitrilase transcripts (Fig. 2a). Furthermore, ISH localization of *BrNIT-T1* and *BrNIT-T2* transcripts using the RNA probes revealed partially overlapping expression patterns on root sections of healthy and clubroot tissues, whereas the patterns obtained using LNA probes were clearly distinct (Figs. 3 and 4). Thus, LNA-modified DNA probes for ISH have clear advantages for discriminating highly similar target sequences.

Isoform-Specific Localization of *BrNIT-T* Transcripts in Clubroot Tissue

ISH analysis using LNA-modified probes demonstrated that the isoform-specific localization of *BrNIT-T* transcripts in *P. brassicae*-infected roots was dependent on the developmental stage of the pathogen (Figs. 4, 5, 6). In the early-growing clubroot (15–20 dag), *BrNIT-T1* transcripts were found over the entire region of the cortex cells of infected roots. In addition, the signal intensity was significantly stronger compared to that in healthy root which was restricted to the pericycle. Subsequently, the *BrNIT-T1* signal was gradually diminished in pathogen-free cells at 30 dag, whereas the strong signal was retained in pathogen-containing cells. In contrast, the *BrNIT-T2* signal, which was observed strongly in noninfected roots, was significantly reduced throughout the entire region of infected roots. These results strongly suggest that *BrNIT-T1* expression was specifically induced by growing secondary plasmodia. Furthermore, strong IAA immunostaining was observed in plasmodia-containing cells. Although IAA immunostaining does not always indicate the presence of free IAA (see below), this result suggests that *BrNIT-T1* is associated with an increase in the total IAA pool in *P. brassicae*-infected cells via *de novo* IAA synthesis.

We previously demonstrated that *BrNIT-T1* was significantly upregulated in *P. brassicae*-infected roots, but that even the increased *BrNIT-T1* expression in clubroot tissues was not comparable to the constitutive level of *BrNIT-T2* (Ishikawa and others 2007b). The present histological observations support the hypothesis that *BrNIT-T1* is induced in a highly localized area surrounding the growing pathogen, where IAA is effectively synthesized to promote gall formation. The highly localized expression can also account for the relatively low levels of *BrNIT-T1* transcript in whole root tissues.

In maturing clubroot tissues, the pathogen-specific expression of *BrNIT-T1* and localization of IAA were diminished as plasmodia transformed into resting spores, whereas *BrNIT-T2* expression was observed in mature cells containing resting spores as well as in noninfected cells (Fig. 6). These shifts in the distribution of nitrilase expression and the IAA pool may be involved in clubroot maturation and/or disease-related deterioration. However, it is also possible that the shifts represent "recovery" from an abnormal physiological condition caused by growing plasmodia. Further studies are necessary for a more complete understanding of the physiological phenomena involved in clubroot maturation.

Validity and Interpretation of IAA Immunostaining in Clubroot Tissue

We performed immunostaining for IAA to examine the spatial relationship of *BrNIT-T* transcripts with IAA distribution. To our knowledge, this is the first report using IAA immunostaining for elucidation of clubroot disease. Devos and others (2006) employed a GUS-reporter assay using the auxin-inducible *DR5* promoter to study clubroot

in *Arabidopsis*. At present, this approach is the most definitive method for indirect localization of free IAA, but it is not applicable to all Brassica plants such as turnip, for which it is difficult to generate transgenic plants. In this respect, immunostaining using commercially available monoclonal antibodies is easily applicable to all plants and requires much less time than generating transgenic plants. However, the immunological approach to estimating free IAA has two disadvantages because the detection system recognizes IAA in its protein-conjugated form. Firstly, free IAA is covalently bound to cellular proteins by prefixation prior to sectioning and detection, leaving open the possibility that immunostaining may identify not only free IAA but also endogenous protein/peptide-conjugated forms of IAA (Walz and others 2002). Secondly, cross-reactivity of the antibody to amino acid-conjugated forms such as IAA-Gly may also be problematic, because amino acid conjugates as well as free IAA are prefixed to cellular proteins via formation of peptide bonds between the carboxylic group of IAA or IAA conjugates and amino groups of proteins. This can be addressed by performing a control experiment omitting the IAA prefixation step. We verified that no signal was observed in non-prefixed sections of noninfected or infected roots (data not shown). Secondly, cross-reactivity of the antibody to amino acid-conjugated forms such as IAA-Gly may also be problematic, because amino acid conjugates as well as free IAA are prefixed to cellular proteins via formation of peptide bonds between the carboxylic group of IAA or IAA conjugates and amino groups of proteins. Unfortunately, the second possibility is unable to be addressed by such control experiments. In addition, we previously discovered that conjugated IAA accumulates in turnip root infected with *P. brassicae* (Ishikawa and others 2007b). Thus, the immunostaining observed in this study may result from conjugated IAA as well as free IAA. Whatever the case, it was obvious that the IAA pool, based on immunostaining, increased in pathogen-infected cells, where *BrNIT-T1* or *BrNIT-T2* transcripts specifically accumulated during the clubroot exponential growth and maturation stages, respectively. This supports the role of nitrilases in IAA biosynthesis, which is crucial for disease development. Further analysis of the molecular species of the accumulated conjugated IAA will be required to fully understand the role of IAA metabolism in clubroot disease.

Physiological Roles of *BrNIT-T* Isoforms

BrNIT-T1 was generally expressed in most young growing tissues of the aerial parts of the plant that are estimated to be major sources of IAA, including the cotyledon, expanding leaf, and flower tissues (Fig. 1). On the other hand, *BrNIT-T1* expression was much lower in root and

hypocotyl compared with *BrNIT-T2* expression, although free IAA was abundant in these tissues (Ishikawa and others 2007a). Based on these findings, we had previously proposed that the physiological function of *BrNIT-T2* in root was to produce IAA (Ishikawa and others 2007b). However, our current analysis of *BrNIT-T* by ISH and IAA by immunostaining demonstrated that transcripts of *BrNIT-T1*, but not *BrNIT-T2*, colocalized with IAA in the pericycle and lateral root-forming sites of healthy roots (Figs. 3, 5, 6, 7). In addition, *BrNIT-T1* transcripts also colocalized with IAA in growing clubroot tissues (Figs. 4, 5, 6, 7). These observations suggest that *BrNIT-T1* is closely involved with IAA synthesis in sites where IAA production is high.

We observed the colocalization of *BrNIT-T1* transcripts and IAA immunostaining in lateral root-forming sites of healthy turnip root. IAA is well known to play a vital role in lateral root initiation and development (Fukaki and Tasaka 2009). Although a large amount of IAA is transported from shoot (apical meristem and young leaves) to root, IAA is also synthesized via the Trp-dependent pathway in *Arabidopsis* root, particularly in root tips and lateral root-forming sites (Müller and others 1998; Ljung and others 2005). Notably, a number of *Arabidopsis* enzymes involved in predicted IAA biosynthetic pathways, including AtNIT1, are specifically expressed in root tips and lateral root-forming sites (Bartel and Fink 1994; Müller and others 1998; Birnbaum and others 2003; Ljung and others 2005). In addition, Kutz and others (2002) reported that AtNIT3 expression is upregulated in lateral root-forming sites of sulfur-starving *Arabidopsis*. These findings suggest that IAA biosynthesis is highly organized within specific root areas which are involved in IAA distribution and development of root architecture. Our results in the present study support that BrNIT-T1 also has a role in the localized IAA production in the formation of lateral root in turnip.

In contrast to *BrNIT-T1* transcripts, *BrNIT-T2* transcripts were highly abundant in healthy root but did not overlap IAA distribution except in cells containing mature resting spores, suggesting that *BrNIT-T2* has a different role from IAA biosynthesis in root. Previous analyses of enzyme activity showed that these turnip nitrilases (like other Brassicaceae nitrilases) have wide substrate specificities toward aliphatic and aromatic nitriles, suggesting additional roles in metabolizing a wide spectrum of compounds (Ishikawa and others 2007b). Such nitriles could be generated via glucosinolate degradation (Wittstock and Halkier 2002; Vaughn and Berhow 2005). Recently, nitrile-specifier proteins that generate nitriles instead of isothiocyanates as the products of myrosinase-dependent glucosinolate hydrolysis were identified, and a biological function of the biased nitrile production was proposed as

promotion of defense against herbivores by affecting oviposition and attracting the specific parasitoid (Mumm and others 2008; Burow and others 2009; Kissen and Bones 2009). However, there is no evidence to date that Brassicaceae nitrilases degrade aliphatic and aromatic nitriles in vivo. Profiling of endogenous nitriles and loss-of-function analysis of nitrilases will be necessary to better understand the overall physiological functions of nitrilase isoforms in metabolism of nitriles in glucosinolate-containing plants.

Plant Hormones May Serve as Regulators for Isoform-Specific Expression of Turnip Nitrilases in Clubroot Disease

Treatment with CK and jasmonic acid (JA) specifically upregulated *BrNIT-T1* and *BrNIT-T2*, respectively (Fig. 8). CK is synthesized by isolated *P. brassicae* secondary plasmodia (Müller and Hilgenberg 1986). In addition, our histochemical analyses demonstrated that *BrNIT-T1* expression and IAA accumulation occurred specifically in cells containing secondary plasmodia. These results suggest that CK originating from the secondary plasmodia may trigger IAA overproduction via induction of *BrNIT-T1*
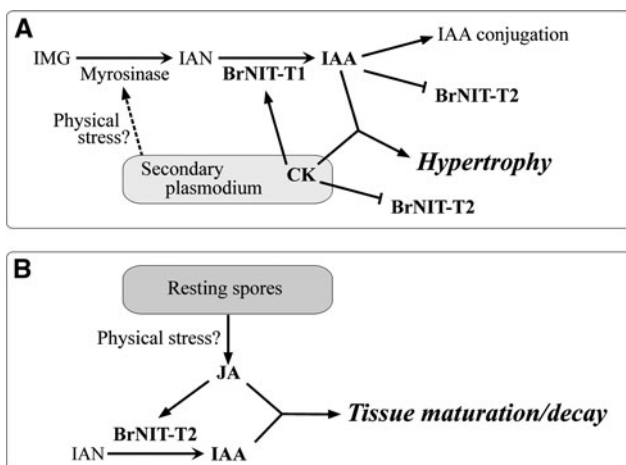
Fig. 9 A schematic model for the roles of *B. rapa* nitrilases in phytohormone crosstalk during clubroot disease development. **a** Events occurring in the early growth of clubroot. Cytokinin (CK) produced by *P. brassicae* plasmodia (Müller and Hilgenberg 1986) upregulates *BrNIT-T1* expression (Figs. 5, 8). Increases in myrosinase (Grsic and others 1999) and *BrNIT-T1* (Ishikawa and others 2007b) result in high production of IAA (Ishikawa and others 2007b) from indole-3-methyglucosinolate (IMG) and indole-3-acetonitrile (IAN) in and around infected cells. Copresence of IAA and CK promotes abnormal cell division and expansion in infected tissues, resulting in clubroot formation. A high level of free IAA and/or CK also induces IAA conjugation and suppresses expression of *BrNIT-T2*, which is the constitutive nitrilase in turnip roots (Ishikawa and others 2007b; Figs. 6, 8). **b** In the later phase of clubroot development, the level of jasmonic acid (JA) is elevated (Grsic and others 1999) by physical stress or signals from mature resting spores. JA stimulates *BrNIT-T2* expression (Fig. 8) and IAA synthesis. Finally, mature *P. brassicae* resting spores are released from decayed tissues to soil

expression. This is consistent with the results by Devos and others (2006) that CK accumulation preceded that of auxin in *P. brassicae*-inoculated *Arabidopsis*.

Grsic and others (1999) reported that endogenous levels of free JA increased at a late stage of clubroot development in Chinese cabbage (*B. rapa*) and that treatment with exogenous JA enhanced nitrilase enzyme activity. These observations, together with our results, lead us to hypothesize that at a late stage of clubroot development, accumulated JA induces *BrNIT-T2* expression. The reason for the accumulation of JA is unclear but may be due to physical stress from the fully expanding pathogen. The increased levels of IAA and JA may be involved in tissue senescence and deterioration, allowing release of mature resting spores into the soil. Figure 9 illustrates a plausible model to explain the isoform-specific roles of *B. rapa* nitrilases in the phytohormone crosstalk required for clubroot formation and maturation.

In conclusion, our histochemical approaches demonstrated the spatiotemporal association between increased *BrNIT-T1* expression, IAA accumulation, and growth of clubroot plasmodia in the early phase of disease development. Although these data strongly suggest that *BrNIT-T1* plays a crucial role in clubroot development via IAA production, it remains to be proven that the transcriptional increase of *BrNIT-T1* is directly linked to elevated enzyme activity and IAA production. Our future challenge is to develop transgenic plants with altered levels of *BrNIT-T* expression to gain more insight into the molecular basis of clubroot development and nitrilase functions.

References

Ando S, Tsushima S, Tagiri A, Kamachi S, Konagaya K, Hagio T, Tabei Y (2006) Increase in *BrAO1* gene expression and aldehyde oxidase activity during clubroot development in Chinese cabbage (*Brassica rapa* L.). Mol Plant Pathol 7:223–234

Bartel B, Fink GR (1994) Differential regulation of an auxin-producing nitrilase gene family in *Arabidopsis thaliana*. Proc Natl Acad Sci USA 91:6649–6653

Bestwick LA, Grønning LM, James DC, Bones A, Rossiter JT (1993) Purification and characterization of a nitrilase from *Brassica napus*. Physiol Plant 89:811–816

Birnbaum K, Shasha DE, Wang JY, Jung JW, Lambert GM, Galbraith DW, Benfey PN (2003) A gene expression map of the *Arabidopsis* root. Science 302:1956–1960

Bischoff M, Löw R, Grsic S, Rausch T, Hilgenberg W, Ludwig-Müller J (1995) Infection with the obligate biotroph *Plasmodiophora brassicae*, the causal agent of club root disease, does not affect expression of NIT1/2-related nitrilases in roots of Chinese cabbage. J Plant Physiol 147:341–345

Burow M, Losansky A, Müller R, Plock A, Kliebenstein DJ, Wittstock U (2009) The genetic basis of constitutive and herbivore-induced ESP-independent nitrile formation in *Arabidopsis*. Plant Physiol 149:561–574

Dekhuijzen HM (1981) The occurrence of free and bound cytokinins in plasmodia of *Plasmodiophora brassicae* isolated from tissue cultures of clubroots. Plant Cell Rep 1:18–20

Devos S, Laukens K, Deckers P, Van Der Straeten D, Beeckman T, Inzé D, Van Onckelen H, Writters E, Prinsen E (2006) A hormone and proteome approach to picturing the initial metabolic events during *Plasmodiophora brassicae* infection on *Arabidopsis*. Mol Plant Microbe Interact 19:1431–1443

Fukaki H, Tasaka M (2009) Hormone interactions during lateral root formation. Plant Mol Biol 69:437–449

Grsic S, Kirchheim B, Pieper K, Fritsch M, Hilgenberg W, Ludwig-Müller J (1999) Induction of auxin biosynthetic enzymes by jasmonic acid and in clubroot diseased Chinese cabbage plants. Physiol Plant 105:521–531

Grsic-Rausch S, Kobelt P, Siemens JM, Bischoff M, Ludwig-Müller J (2000) Expression and localization of nitrilase during symptom development of the clubroot disease in *Arabidopsis*. Plant Physiol 122:369–378

Ishikawa T, Kuroda H, Okazaki K, Itoh K, Mitsui T, Hori H (2007a) Evaluation of roles of amidase which converts indole-3-acetamide to indole-3-acetic acid, in formation of clubroot in turnip. Bull Fac Agr Niigata Univ 60:53–60

Ishikawa T, Okazaki K, Kuroda H, Itoh K, Mitsui T, Hori H (2007b) Molecular cloning of *Brassica rapa* nitrilases and their expression during clubroot development. Mol Plant Pathol 8:623–637

Kissen R, Bones AM (2009) Nitrile-specifier proteins involved in glucosinolate hydrolysis in *Arabidopsis thaliana*. J Biol Chem 284:12057–12070

Koshkin AA, Rajwanshi VK, Wengel J (1998a) Novel convenient syntheses of LNA [2.2.1]bicycle nucleosides. Tetrahedron Lett 39:4381–4384

Koshkin AA, Singh SK, Nielsen P, Rajwanshi VK, Kumar R, Meldgaard M, Olsen CE, Wengel J (1998b) LNA (Locked nucleic acids): synthesis of the adenine, cytosine, guanine, 5-methylcytosine, thymine and uracil bicyclonucleoside monomers, oligomerisation, and unprecedented nucleic acid recognition. Tetrahedron 54:3607–3630

Kutz A, Müller A, Hennig P, Kaiser WM, Piotrowski M, Weiler EW (2002) A role for nitrilase 3 in the regulation of root morphology in sulphur-starving *Arabidopsis thaliana*. Plant J 30:95–106

Laemmli UK (1970) Cleavage of structural proteins during the assembly of the head of bacteriophage T4. Nature 227:680–685

Ljung K, Hull AK, Celenza J, Yamada M, Estelle M, Normanly J, Sandberg G (2005) Sites and regulation of auxin biosynthesis in Arabidopsis roots. Plant Cell 17:1090–1104

Moctezuma E (1999) Changes in auxin patterns in developing gynophores of the peanut plant (*Arachis hypogaea* L.). Ann Bot 83:235–242

Müller P, Hilgenberg W (1986) Isomers of zeatin and zeatin riboside in clubroot tissue: evidence for *trans*-zeatin biosynthesis by *Plasmodiophora brassicae*. Physiol Plant 66:245–250

Müller A, Hillebrand H, Weiler EW (1998) Indole-3-acetic acid is synthesized from L-tryptophan in roots of *Arabidopsis thaliana*. Planta 206:362–369

Mumm R, Burow M, Bukovinszkine'Kiss G, Kazantzidou E, Wittstock U, Dicke M, Gershenzon J (2008) Formation of simple nitriles upon glucosinolate hydrolysis affects direct and indirect defense against the specialist herbivore, *Pieris rapae*. J Chem Ecol 34:1311–1321

Neuhaus K, Grsic-Rausch S, Sauerteig S, Ludwig-Müller J (2000) *Arabidopsis* plants transformed with nitrilase 1 or 2 in antisense direction are delayed in clubroot development. J Plant Physiol 156:756–761

Normanly J, Grisafi P, Fink GR, Bartel B (1997) *Arabidopsis* mutants resistant to the auxin effects of indole-3-acetonitrile are defective in the nitrilase encoded by the *NIT1* gene. Plant Cell 9:1781–1790

Obika S, Nanbu D, Hari Y, Andoh J, Morio K, Doi T, Imanishi T (1998) Stability and structural features of the duplexes containing nucleoside analogues with a fixed N-type conformation, 2′-O, 4′-C-methyleneribonucleosides. Tetrahedron Lett 39:5401–5404

Rausch T, Butcher DN, Hilgenberg W (1981) Nitrilase activity in clubroot diseased plants. Physiol Plant 51:467–470

Silahtaroglu A, Pfundheller H, Koshkin A, Tommerup N, Kauppinen S (2004) LNA-modified oligonucleotides are highly efficient as FISH probes. Cytogenet Genome Res 107:32–37

Simeonov A, Nikiforov TT (2002) Single nucleotide polymorphism genotyping using short, fluorescently labeled locked nucleic acid (LNA) probes and fluorescence polarization detection. Nucleic Acids Res 30:e91

Ugajin T, Takita K, Takahashi H, Muraoka S, Tada T, Mitsui T, Hayakawa T, Ohyama T, Hori H (2003) Increase in indole-3-acetic acid (IAA) level and nitrilase activity in turnips induced by *Plasmodiophora brassicae* infection. Plant Biotechnol 20:215–220

Válóczi A, Hornyik C, Varga N, Burgyan J, Kauppinen S, Havelda Z (2004) Sensitive and specific detection of microRNAs by northern blot analysis using LNA-modified oligonucleotide probes. Nucleic Acids Res 32:e175

Válóczi A, Varallyay E, Kauppinen S, Burgyan J, Havelda Z (2006) Spatio-temporal accumulation of microRNAs is highly coordinated in developing plant tissues. Plant J 47:140–151

Vaughn SF, Berhow MA (2005) Glucosinolate hydrolysis products from various plant sources: pH effects, isolation, and purification. Ind Crop Prod 21:193–202

Vorwerk S, Biernacki S, Hillebrand H, Janzik I, Müller A, Weiler EW, Piotrowski M (2001) Enzymatic characterization of the recombinant *Arabidopsis thaliana* nitrilase subfamily encoded by the *NIT2/NIT1/NIT3*-gene cluster. Planta 212:508–516

Walz A, Park S, Slovin JP, Ludwig-Müller J, Momonoki YS, Cohen JD (2002) A gene encoding a protein modified by the phytohormone indoleacetic acid. Proc Natl Acad Sci USA 99:1718–1723

Wittstock U, Halkier BA (2002) Glucosinolate research in the *Arabidopsis* era. Trends Plant Sci 7:263–270